

PACS numbers: 42.55.Lt; 42.60.By; 42.60.Lh
DOI: 10.1070/QE2004v034n09ABEH002687

A 2-kJ wide-aperture XeCl laser

S.P. Bugaev, E.N. Abdullin, V.B. Zorin, B.M. Koval'chuk, S.V. Loginov, G.A. Mesyats, V.S. Skakun, V.F. Tarasenko, V.S. Tolkachev, P.M. Shchanin

***Abstract*. A 308-nm XeCl laser with an active volume of 600 L is studied experimentally. The laser is pumped by a radially convergent electron beam from an accelerator with vacuum insulation. The output energy of 1.9 kJ and power of ~ 7 GW are achieved upon pumping the Ar – Xe – HCl mixture. The laser pulse FWHM is ~ 250 ns.**

Keywords: *XeCl laser, electron-beam pumping, lasing energy*.

1. Introduction

Research and development of high-power laser systems using exciplex lasers operating on halides of inert gases are being pursued at present [1 – 5]. The laser systems consist of a master oscillator and several amplifiers. The final amplifier is usually an electron-beam-pumped wide-aperture laser [1 – 7]. In most of the wide-aperture electron-beam-pumped exciplex lasers [1 – 4, 6], high pump powers were achieved by using intermediate water lines charged by pulsed generators. The use of an additional energy accumulator complicates the laser design.

In electron accelerators developed at the Institute of High-Current Electronics, Siberian Branch, Russian Academy of Sciences, Tomsk, the inductances of the pump generator and the vacuum diode were reduced considerably by using vacuum insulation [8, 9]. This made it possible to design compact wide-aperture exciplex lasers [5, 10 – 12] directly pumped by Marx generators with vacuum insulation. These lasers were excited by four [5, 10] and six [5, 11, 12] radially convergent beams.

In this work, we carry out detailed investigations of a wide-aperture XeCl laser pumped by a radially converging electron beam. In this laser, a single-loop pump generator circuit is used owing to vacuum isolation.

2. Laser design and measuring technique

Figure 1 shows the setup. The accelerating complex of the device contains 12 vacuum diodes fed by 12 pulsed voltage generators (PVGs) and arranged in accordance with the design of a two-tier six-point star [9]. Cathodes with a smooth emitting surface made of PU carbotextim and covered with velvet are used in accelerating modules. Electron beams from all the accelerating modules are injected into the gas volume of the laser chamber through a system of partition windows fastened to a tube with an outer diameter 62 cm. The residual pressure in the casing of the accelerator did not exceed 2×10^{-3} Pa for an excess pressure up to 3 atm in the laser chamber. This was achieved due to the simultaneous operation of three vacuum AVP-400/1600 pumps, each having a pump rate of 3000 L s^{-1}.

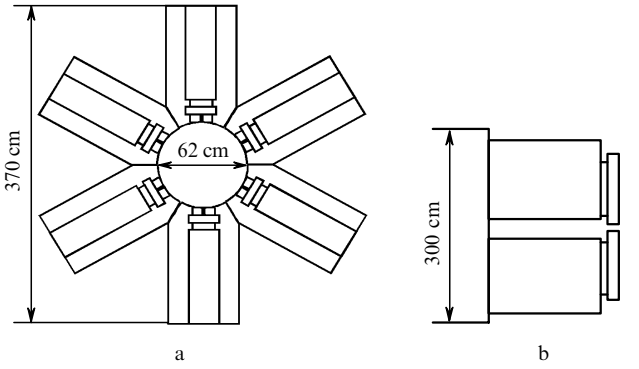

Figure 1. Scheme of the setup: (a) cross section of six PVGs and (b) longitudinal two-tier arrangement of PVGs.

The switches of all the 12 PVGs (96 in all) operated on a 70 : 30 mixture of dry air and sulphur hexafluoride under a total pressure 1.3 – 1.7 atm, and the capacitors were charged to a voltage 70 – 95 kV. The PVGs were controlled using 12 air-filled multiple spark gaps and an equal number of coaxial-cable pulsed transformers. The spread in the operation time of PVGs did not exceed 100 ns. The output voltage of each PVG was ~ 0.6 MV and the current of 60 kA. Accordingly, the total current of 12 PVGs was 720 kA. The voltage pulse front did not exceed 0.2 μs for the pulse FWHM of ~ 0.5 μs.

The system of foil partition windows had a complicated construction and was made on a common frame, a system of 12 support grids and the foils themselves, fastened by a bracing mechanism. Titanium foil of thickness 40 μm was used in the system. The total area of the foil window was ~ 3 m^2, the geometrical transparency of the support grid alone was ~ 80 %, while the overall transparency was ~ 70 %.

S.P. Bugaev, E.N. Abdullin, V.B. Zorin, B.M. Koval'chuk, S.V. Loginov, G.A. Mesyats, V.S. Skakun, V.F. Tarasenko, V.S. Tolkachev, P.M. Shchanin Institute of High-Current Electronics, Siberian Branch, Russian Academy of Sciences, prosp. Akademicheskii 4, 634055 Tomsk, Russia; e-mail: VFT@loi.hcei.tsc.ru

Received 6 April 2004
Kvantovaya Elektronika **34** (9) 801 – 804 (2004)
Translated by Ram Wadhwa

The diameter of the active region was 60 cm, its length was 200 cm, the active volume was 600 L, and the overall volume was 980 L. The distance between two plane internal mirrors was 335 cm. For the totally reflecting mirror, we used a mirror with a K8 glass substrate covered with aluminium coating. The output mirror was in the form of a plane–parallel quartz plate. Figure 2 shows a photograph of the laser from which radiation was extracted vertically downwards.

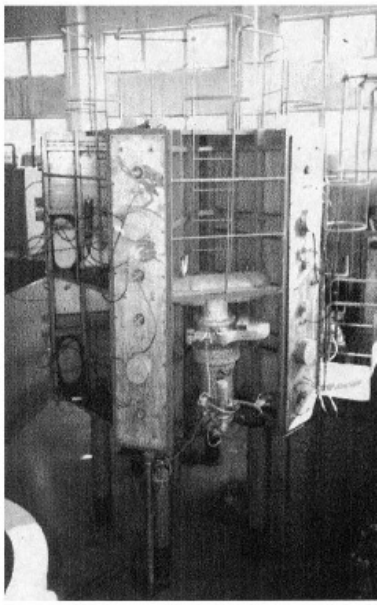

Figure 2. Wide-aperture laser with an active volume of 600 L pumped by 12 electron beams.

The electron beam energy transferred to the gas was determined from the increase in the laser chamber pressure following the electron beam injection. A pressure pulse was detected by a gauge based on a 6MDKh-3B mechanotron calibrated using a reference manometer upon a slow variation of pressure in the laser chamber. The input energy obtained in this way corresponded just to the energy spent on heating of the gas. The part of the energy dissipated in the form of radiation through the output mirror, as well as the energy spent on heating of the walls and formation of acoustic waves, was neglected. However, our estimates reveal that no more than 10 % – 20 % energy was lost in this way.

We determined the laser radiation energy and its distribution over the output beam cross section by using an automated measuring system based on TPI-2M.1 calorimetric transducers operating in the energy range 1 – 100 J per calorimeter in the spectral range 0.2 – 20 μm. The working area of the detecting element of a calorimeter was 36 cm^2. To increase the detecting surface area, up to 31 calorimeters were combined into a single block. The energy absorbed by each calorimeter, the energy distribution among calorimeters, and the energy absorbed by the total working surface of the block of calorimeters were recorded for each pulse. Since the admissible density and the radiation power of TPI-2M.1 calorimeters are limited, the IMO-2N and IKT-1 detectors were used for additional calibration of these calorimeters. The energy distribution over the output laser beam cross section was also determined from the autograph on photographic paper, whose darkening upon a change in the radiation energy density was practically linear.

The temporal characteristics of the pump were determined by using voltage dividers and Rogowski loops. Measurements were made simultaneously for all 12 PVGs. Laser radiation pulses were recorded with the help of vacuum photodiodes FEK-22 from which the signals were supplied to the oscillographs C8-14.

The working mixtures consisting of argon, xenon and HCl were prepared directly in the laser chamber which was passivated beforehand.

3. Simulation of accelerator operation

To determine the optimal working conditions for the accelerator, a modular unit was first constructed by using a single vacuum PVG [9, 13]. The scheme of the diode of the accelerator is shown in Fig. 3. The same figure shows the electron trajectories and the corresponding beam current density distributions at the anode for various voltages across the diode, obtained as a result of numerical calculations with the help of the Poisson-2 program package [14]. The electrode gap of the vacuum diode with a smooth cathode was used for obtaining a beam with a cross section of 25 × 100 cm and with an electron energy of 500 – 600 keV. The beam current attained values of 60 kA for a pulse duration of 1.5 – 2.0 μs at the base. The power source was a Marx generator with a vacuum insulation. The cathode was placed in the last stage of the generator; the accelerator did not contain a bushing vacuum insulator. The 190 × 810-mm emitting surface of the cathode was prepared from graphitised carbon felt. The radius of curvature of the supporting grid of the output window was 528 mm. The cathode–anode distance d in the diode symmetry plane was 60 – 65 mm. The rated current density distributions in direction l on the anode surface in the absence of the anode plasma were sufficiently uniform.

Figure 4 shows the oscillograms of voltage and current pulses in the diode, the time dependence of the electron beam power and energy as well as the diode perveance calculated using these oscillograms, and the energy distribution in the electron beam extracted behind the anode foil,

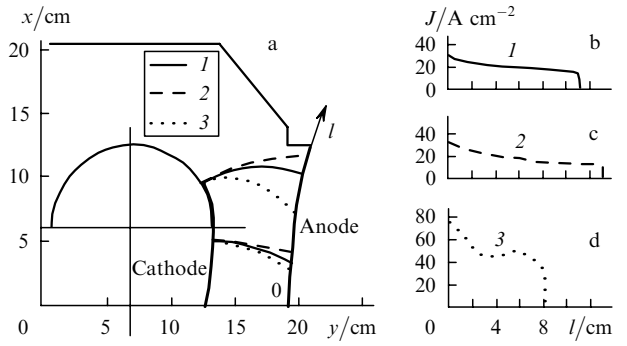

Figure 3. Scheme of the vacuum diode of a PVG (a) and the beam current density distribution at the anode for a voltage U across the vacuum diode equal to 500 (b) and 300 kV (c) as well as in the case of an additionally created anode plasma for $U = 500$ kV (d). Curves (*1* – *3*) in (a) show electron trajectories; l is the coordinate along the anode surface (foil window).

which was recorded in a pulse using TPI-2M.1 calorimeters (48 in all). It can be seen that the voltage and current oscillograms are similar, which indicates an effective power transfer from the generator to the electron beam. The time of perveance stabilisation can be put in correspondence with the time of formation of the plasma emission boundary, which is approximately equal to 50 ns; the diode current appears almost simultaneously with the voltage across the electrode gap. The diode perveance varies insignificantly during the pulse, indicating the invariable position of the plasma emission boundary in the electrode gap during the major part of the voltage pulse.

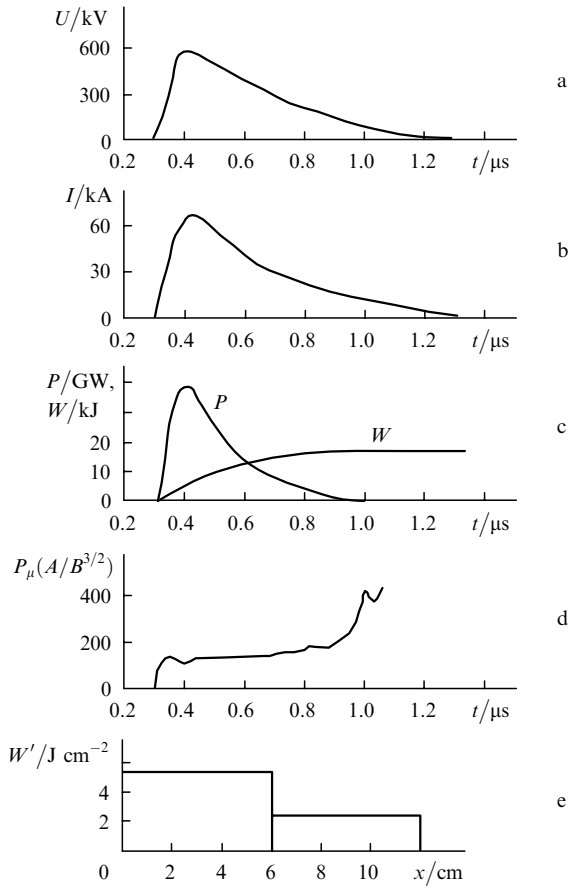

Figure 4. Oscillograms of voltage pulses in a vacuum diode (a) and of beam current (b) for a cathode–anode gap of 60 mm, as well as the time dependences of the beam power and energy (c) and the diode perveance (d) and the energy density distribution in the electron beam extracted behind the anode foil at right angles to the longitudinal axis of the window, obtained with the help of 48 TPI-2M.1 calorimeters arranged in two rows along the foil window (e).

The discrepancy observed between the theoretical beam current density distribution at the diode and the experimentally obtained beam energy distribution behind the anode foil can be due to the presence in the electrode gap of a space charge of gas ions desorbed from the anode, which was disregarded in numerical analysis. The rated value of the current for a voltage of 600 kV across the diode and an electrode gap of 60 mm is 47 kA, which is also noticeably lower than the experimental value. The total beam energy in the diode is ~ 17 kJ, the energy behind the foil is ~ 10 kJ, while the energy stored in the Marx generator is ~ 22 kJ. It was noted above that 12 such PVGs were used for pumping the laser, and any number of such units (from 1 to 12) could be actuated simultaneously irrespective of their arrangement.

4. Experimental results on lasing and discussion

We have studied the effect of the pressure and composition of the working mixture, charging voltage, and the number of PVGs actuated in the setup on the lasing parameters of an HCl laser, as well as the dependence of radiation energy on the number of pulses and operation time for a single portion of the mixture. The distribution of the radiation energy over the output beam cross section was also studied. The data obtained in this way are illustrated in Figs 5–8.

The radiation energy increases by 30% as the working pressure increases from 1 to 1.5 atm, while the corresponding increase upon a pressure increase from 1.5 to 2 atm is just 20 % (see Fig. 5). This is due to the fact that, for a charging voltage $U_0 = 85$ kV, the main part of the electron beam energy is supplied to the working mixture, and only a small part of the energy reaches the opposite wall. Accordingly, the energy contribution to the working mixture varies insignificantly as the pressure increases from 1.5 to 2 atm.

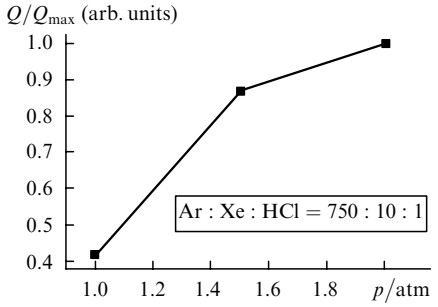

Figure 5. Relative radiation energy of the laser as a function of the pressure in the Ar–Xe–HCl mixture for a charge voltage $U_0 = 85$ kV.

Figure 6 shows the dependences of the radiation energy on the number of PVGs actuated for two mixtures with different compositions of the constituent gases. For a comparatively low concentration of Xe and HCl, the increase in the pump power associated with the number of PVGs leads to a decrease in the radiation energy, while the highest radiation energies are attained for small pump power in mixtures with an optimal concentration of the constituent gases. The dependence shown in Fig. 4 was

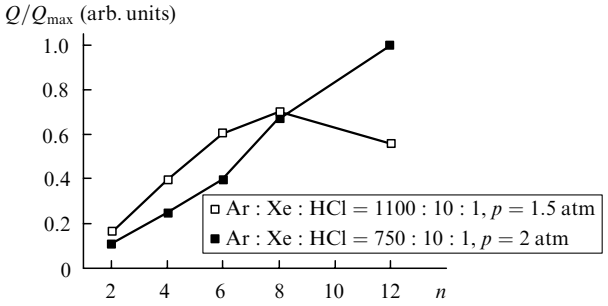

Figure 6. Dependence of the relative radiation energy of the laser on the number n of actuated PVGs for different gas mixtures and pressures at $U_0 = 85$ kV.

obtained for a charge voltage of 85 kV. Mixtures with a higher concentration of Xe and HCl should be used for a further increase in the pump power due to the charging voltage.

Figure 7 shows the dependence of the radiation energy and efficiency on the energy supplied to the Ar : Xe : HCl = 750 : 10 : 1 mixture for $U_0 = 85$ kV. The maximum radiation energy was 1.6 kJ for an efficiency 3.8 % of the energy supplied to the working mixture. In this case, the radiation pulse duration was ~ 250 ns and its delay relative to the beginning of the beam current pulse was ~ 100 ns. As the charging voltage in the Ar : Xe : HCl = 750 : 25 : 1 mixture was increased to 95 kV, the radiation energy assumed the value 1.9 kJ at a pressure of 2 atm. The radiation energy distribution in the output beam was different in two directions in view of a small wedge formed by the surfaces of the output quartz plate. The nonuniformity in the radiation energy distribution along the axis perpendicular to the wedge was less than 10 %.

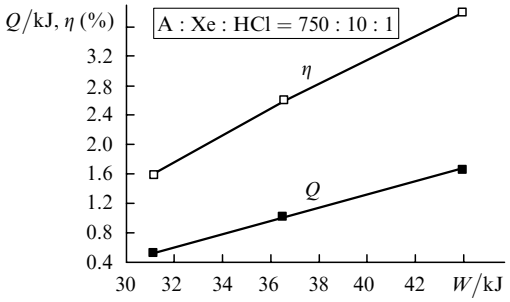

Figure 7. Dependences of the radiation energy of the laser and the efficiency on the energy supplied to the gas and determined from the pressure jump for the Ar–Xe–HCl mixture for $U_0 = 85$ kV.

The maximum radiation energies are achieved in the first pulses. After 3–5 switchings, the radiation energy is stabilised at a level of 80 % of the first pulse energy and then remains unchanged for a long time. Figure 8 shows the dependence of the radiation energy per pulse on the number of laser pulses and the operation time for one portion of the mixture after the attainment of steady-state conditions. The difference in the radiation energies of the 13th and 41st pulses was only ~ 20 % for operation with one portion of the mixture for 146 h. Because of an increase in the ratio of the inner surface of the laser chamber to its volume, a more rapid degradation of the working mixture was observed in such a laser with an active volume of about 30 L [10]. Our experiments were carried out for the same specific energy contribution, the same mixtures and the same pressures, and for the same preset ratio between the active and total volumes of the laser chamber as in [10].

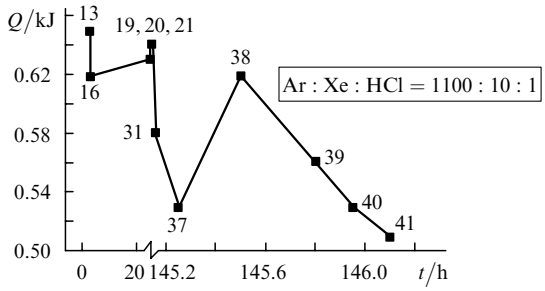

Figure 8. Dependence of the radiation energy per pulse on the number of pulses and the operation time for a portion of the Ar–Xe–HCl mixture for $U_0 = 85$ kV and $p = 1.5$ atm. The figures at the symbols indicate the pulse number.

The fraction of IR laser radiation spent on Xe atomic transitions was less than 1 % of the total radiation under optimal conditions for the given XeCl laser at a wavelength of 308 nm. Even for IR generation alone in an Ar–Xe mixture, the radiation energy spent on Xe atomic transitions for a specific pump power of ~ 100 kW cm^{-3} did not exceed 10 J, and the lasing efficiency was below 0.05 % [12].

5. Conclusions

Thus, the analysis of a high-power wide-aperture XeCl laser with an active volume of 600 L has shown that a radiation energy of 1.6 kJ was achieved in the Ar : Xe : HCl = 750 : 10 : 1 mixture under a pressure of 2 atm for $U_0 = 85$ kV at $\lambda \sim 308$ nm, while the corresponding radiation energy for $U_0 = 95$ kV was 1.9 kJ. Owing to the injection of an electron beam into such a laser from six sides, a uniform distribution of radiation energy over the output beam cross section was obtained. The large value of the ratio of the volume of the laser chamber to the area of its inner surface has made it possible to work with the same portion of the working mixture. Owing to the one-loop scheme of the pump generator, the laser studied here is distinguished by simplicity of construction and a comparatively small size.

Acknowledgements. The authors thank G.P. Belov, L.G. Vintizenko, S.I. Gorbachev, V.M. Zaslavskii, A.M. Efremov, S.V. Ivanov, V.N. Kiselev, Yu.S. Korenblit, V.F. Losev, A.A. Novikov, Yu.V. Perchin, A.V. Fedenev, E.A. Fomin, and V.T. Shkatov for their help in carrying out this research.

References

1. Shaw M.J. *Proc. SPIE Int. Soc. Opt. Eng.*, **3092**, 154 (1997).
2. Sethian J.D., Pawley C.J., Obenschain S.P., et al. *IEEE Trans. Plasma Sci.*, **25**, 221 (1997).
3. Owadano Y., Okuda I., Matsumoto Y., et al. *Fusion Engineering and Design*, **44**, 91 (1999).
4. Zvorykin V.D., Arlantsev S.V., Bakaev V.G., et al. *Laser and Particle Beams*, **19**, 609 (2001).
5. Koval'chuk B.M., Losev V.F., Mesyats G.A., Tarasenko V.F. *Izv. Vyssh. Uchebn. Zaved. Ser. Fiz.*, (5), 12 (2000).
6. Rosocha L.A., Hanlon J.A., McLeond J., et al. *Fusion Technol.*, **11**, 576 (1987).
7. Abdullin E.N., Grishin D.M., Gubanov V.P., et al. *Kvantovaya Elektron.*, **34**, 199 (2004) [*Quantum Electron.*, **34**, 199 (2004)].
8. Mesyats G.A., Bychkov Yu.I., Kovalchuk B.M. *Proc. SPIE Int. Soc. Opt. Eng.*, **1628**, 70 (1992).
9. Abdullin E.N., Bugaev S.P., Efremov A.M., et al. *Prib. Tekh. Eksp.*, (5), 138 (1993).
10. Abdullin E.N., Gorbachev V.I., Efremov A.M., et al. *Kvantovaya Elektron.*, **20**, 652 (1993) [*Quantum Electron.*, **23**, 564 (1993)].
11. Mesyats G.A., Osipov V.V., Tarasenko V.F. *Pulsed Gas Lasers* (Washington: SPIE PRESS, 1995).
12. Koval'chuk B.M., Tarasenko V.F., Fedenev A.V. *Kvantovaya Elektron.*, **23**, 504 (1996) [*Quantum Electron.*, **26**, 489 (1996)].
13. Abdullin E.N., Belomytsev S.Ya., Bugaev S.P., et al. *Fiz. Plazm.*, **17**, 741 (1991).
14. Astrelin V.T., Ivanov V.Ya. *Avtometriya*, (3), 92 (1980).